

Mg II h&k line diagnostics of IM Pegasi^{*}

K. Oláh¹, D. Marik¹, E. R. Houdebine², R. C. Dempsey^{3,**,***}, and E. Budding⁴

¹ Konkoly Observatory of the Hungarian Academy of Sciences, H-1525 Budapest, Hungary
(e-mail: olah@ogyalla.konkoly.hu, dmarik@ogyalla.konkoly.hu)

² Space Science Department, ESA-ESTEC Postbus 299, 2200 AG Noordwijk, and Sterrenkundig Instituut, Kruislaan 403, 1098 SJ Amsterdam, The Netherlands

³ Astronomy Programs, Computer Sciences Corporation, Space Telescope Science Institute, 3700 San Martin Drive, Baltimore, MD 21218, USA

⁴ Central Institute of Technology, P.O. Box 40740, Upper Hutt, Wellington, New Zealand; Carter Observatory, P.O. Box 2909, Wellington C.1., New Zealand

Received 18 December 1996 / Accepted 8 October 1997

Abstract. We have analysed the Mg II h&k resonance lines of IM Peg (KII-III) on 14 high resolution IUE LWR spectra and compared the results coming from visual spectroscopic and $UBV(RI)_C$ photometric data. The ‘clean’ spectra (free from interstellar absorption) were modelled using a convolution of the rotational profile with a Gaussian profile, that represents macroturbulence and broadenings of other origin, the former dominating.

Significant variations in the h&k line fluxes and widths were found throughout the orbital phase range. A line broadening effect is found at maximum spot visibility both in the k and h lines. The Mg II line widths increase linearly with the flux of the transition region lines as a function of rotational phase. Anticorrelations as a function of phase were found between the Mg II line fluxes and the higher temperature lines. The k line is broader than the h line, correlated with a slope greater than unity, in keeping with a greater radiation transfer effect in the k line, and a non-optically thin medium at all phases. We observe a systematic asymmetry in the ratio of the h to k line profiles at all phases. The spectral diagnostics thus suggest the appearance of a plage region on the stellar disc.

We obtained new orbital elements of the IM Peg system, deriving a small, but non-zero eccentricity.

Key words: stars: individual: IM Peg – stars: activity – stars: chromospheres – stars: binaries: spectroscopic – stars: late-type

Send offprint requests to: K. Oláh

* The authors would like to dedicate this paper to their late referee, Dr. P.B. Byrne.

** Visiting Astronomer, Kitt Peak National Observatory, National Optical Astronomy Observatories, operated by the Association of Universities for Research in Astronomy, Inc., under contract with the National Science Foundation.

*** Guest Investigator with the International Ultraviolet Explorer satellite, which is sponsored and operated by the National Aeronautics and Space Administration, by the the Science Research Council of the United Kingdom, and by the European Space Agency.

1. Introduction

The Mg II h&k resonance lines are well-known activity indicators in late-type stars. Since very early stellar activity studies, chromospheres were investigated using observations and modelling of these lines. Neff (1991) described in detail how the ultraviolet spectral imaging method could help in studying the chromospheres of late-type active stars. A classic example of this research was carried out by Neff et al. (1989). The basic idea was, that if there is a non-uniform emission source on the stellar surface, an additional component is needed to model the spectral line beside the symmetric one centered at the stellar velocity, assumed to be Gaussian. However, previous studies on mapping stellar surfaces did not take into account line profile broadening mechanisms other than rotation. Instead, targets were appropriately chosen so that the major part of the line broadening was due to rotation and the other effects were assumed negligible. Oláh et al. (1992) described a method to separate the rotational broadening of the Mg II h&k line profiles from broadening caused by other factors. In the case of HK Lac (KOIII+?), Oláh et al. (1992) found that broadening due to rotation was comparable to another broadening mechanism that is unknown in detail, but assumed to be due to the effects of turbulence in the line forming medium.

A similar, two-Gaussian approach has been used on other RS CVn systems (e.g., Wood et al. (1995); Dempsey et al. (1996b)). In those studies, the Mg II profile is fit with a ‘narrow’ and ‘broad’ component. Alternatively, an anisotropic turbulence model has been used successfully to fit the Mg II and C IV profiles of V824 Arae (Dempsey et al. (1997)). In these approaches, broadening beyond rotation is attributed to either continuous microflaring or asymmetrically distributed radial and tangential macroturbulence.

In the present paper, we apply Oláh et al.'s (1992) analysis technique to the RS CVn system IM Peg (HD 216489), a binary consisting of a K2II-III primary and a companion of unknown spectral type with an orbital period of 24.649 days. Here we use time series observations of the Mg II lines and try to describe the variability of the profiles in terms of the two aforementioned broadening terms. In addition, we also incorporate an optical depth term into our fitting function. We further use the ratio of the line profiles to probe the fluctuations of the optical depth in the chromosphere. Further diagnostic information can be obtained by comparing the Mg II line broadening with the fluxes of transition region lines like Si IV and C IV. Finally, we use the new data to compute a revised orbit for the binary and analyse the IUE data for the presence, if any, of systematic line shifts.

2. IUE observations

We have analysed a series of IUE LWR spectra of the active giant star IM Peg. The spectra cover almost, and were obtained within, one rotational cycle, and have been taken as part of an observing campaign, together with visual spectroscopic and $UBV(RI)_C$ photometric data. At each phase longer exposure (LWP 24134, 24141, 24156, 24171, 24193, 24250, 24290) and shorter exposure (LWP 24135, 24142, 24157, 24172, 24194, 24249, 24291) spectra were obtained. The observing log and further details of the observations and reduction can be found in Dempsey et al. (1996a).

3. Method of the line profile fitting

Altogether, 14 high resolution spectra were used to analyse the Mg II h&k resonance lines. As a first step the interstellar absorption lines were removed from the data. We used two component Gaussian fits to the observations, one for the stellar, another for the interstellar line. Our procedure gives wavelength, peak intensity and FWHM for both the stellar and interstellar components. We note, that the resolution of the IUE HIRES spectra is about 0.2\AA and the derived FWHM of the interstellar (IS) feature is not much wider than this ($\approx 0.28\text{\AA}$) in our spectra, so we cannot study the shape of the absorption component. Oláh et al. (1992) demonstrated that, in cases like IM Peg, empirically combining the IS and stellar components as either a product or sum, yields fittings of essentially the same quality. Here we use a sum of two Gaussians for fitting the IS and stellar components. Adding back the fitted IS feature with opposite sign to the data, we constructed 'clean' spectral lines for further modelling. Sums of Gaussians were successfully used for such line profile fitting in several previous similar cases, e.g., for AR Lac by Neff et al. (1989) or for V711 Tau by Dempsey et al. (1996b).

Rotational phases were calculated using the ephemeris $2422243.316 + 24.649 \times E$ (Eaton et al., 1983). The mean wavelength of the h IS feature is $2802.762 \pm 0.051\text{\AA}$ with a mean of $0.256 \pm 0.031\text{\AA}$ FWHM, whereas the k IS is centered at $2795.597 \pm 0.045\text{\AA}$ and has $0.277 \pm 0.023\text{\AA}$ FWHM. The mean fluxes of the h and k IS lines are 0.25 ± 0.03 and

$0.33 \pm 0.05 \cdot 10^{-11} \text{erg s}^{-1} \text{cm}^{-2}$, respectively, which are less than 15% of the stellar line fluxes. The errors are single standard deviations. Taking into account the extreme IS flux values, the subtraction of the IS lines would cause less than 2–3% error in the stellar line fluxes.

The observed profiles and the two component Gaussian fits for 7 spectra (those which had longer exposure times and therefore better signal to noise ratio) are displayed in Fig. 1. Similar results are found for the remaining data. Wavelengths were transformed to a velocity scale using air wavelengths of 2802.705\AA and 2795.528\AA for the h and k lines, respectively. This plot allows us to compare the line profiles of the h&k lines directly. A small discrepancy in the velocity transformation may arise from the fact that the h&k lines appear in different echelle orders of the LWP camera, however, this (systematic) uncertainty does not exceed $2\text{--}3 \text{ km s}^{-1}$ (see Robinson and Carpenter, 1995).

Using our reduced data, keeping in mind the measurement uncertainties, we proceeded with a simple two component fit to the line profiles. Following Oláh et al. (1992), the resulting 'clean' spectra (free from interstellar absorption) were further modelled assuming that the width of the lines came from:

- rotational broadening ('dish-shaped' component): 'r' parameter
- intrinsic broadening (Gaussian component): 's' parameter

The meaning of these parameters has been discussed previously (cf. Oláh et al. 1992). The 'r' parameter, for instance, has a value for a rapid rotation, as in the present case, which is easy to estimate, and determinations in such contexts have been found to be quite robust. The 's' parameter relates generally to other broadening factors. At the temperature of $\approx 8000\text{K}$, where the Mg II h&k lines are formed in a giant star's atmosphere, the thermal broadening is not strong: thermal velocities can be $\approx 2 \text{ km s}^{-1}$ for the line forming ions. Effects associated with the finite atmospheric region of the line's formation around this temperature may contribute to 's'. When we take out the rotational broadening from the profile, what is left, however, is much broader than would follow from such an effect. Therefore, this 's' parameter must reflect processes that randomize motions on a scale several times greater than is possible by a classical, temperature-related process.

Further consideration of our results, and correspondence with the referee, particularly concerning this latter point, led us to extend our fitting procedure to try to take into account such scattering effects. For this purpose we introduced another parameter τ denoting the optical depth of the region in which the line is taken to be predominantly formed. Photons of a frequency near that of the natural centre of the line from such a region can be depleted by scattering encounters with other MgII ions as they emerge from the chromosphere.

The two component profile fitting, considered previously, comes from convolving the dish-shaped rotational form

$$f_1(r, \lambda) = I_b + \frac{3I_0}{(3-u)} \left\{ (1-u)J_1(r, \lambda) + \frac{\pi}{4}J_2(r, \lambda) \right\}, \quad (1)$$

Table 1. Results of the clean fits of the Mg II h & k lines of IM Peg.

LWP	ϕ	k line							h line						
		flux ^a	τ	<i>r</i>	<i>s</i>	<i>I</i> (p) ^b	FWHM	λ	flux ^a	τ	<i>r</i>	<i>s</i>	<i>I</i> (p) ^b	FWHM	λ
24134	0.18	2.11	0.78	<i>0.29</i>	0.73	3.11	1.323	2795.177	1.68	0.77	<i>0.27</i>	0.62	2.38	1.238	2802.330
24135	0.18	2.20	0.80	<i>0.29</i>	0.73	3.03	1.354	2795.222	1.55	0.79	<i>0.27</i>	0.60	2.25	1.192	2802.389
24141	0.26	2.28	0.80	<i>0.28</i>	0.73	3.17	1.345	2795.240	1.69	0.80	<i>0.27</i>	0.58	2.33	1.205	2802.391
24142	0.26	2.36	0.80	<i>0.28</i>	0.70	3.29	1.316	2795.222	1.80	0.79	<i>0.27</i>	0.60	2.50	1.216	2802.356
24156	0.34	2.34	0.80	<i>0.29</i>	0.75	3.21	1.400	2795.291	1.74	0.79	<i>0.27</i>	0.65	2.40	1.294	2802.422
24157	0.34	2.16	0.80	<i>0.29</i>	0.79	3.08	1.411	2795.336	1.68	0.79	<i>0.28</i>	0.68	2.42	1.296	2802.496
24171	0.42	2.14	0.80	<i>0.29</i>	0.80	3.12	1.447	2795.393	1.79	0.79	<i>0.27</i>	0.65	2.47	1.244	2802.544
24172	0.42	2.17	0.81	<i>0.31</i>	0.86	3.01	1.503	2795.449	1.72	0.78	<i>0.28</i>	0.68	2.37	1.314	2802.623
24193	0.50	2.20	0.82	<i>0.32</i>	0.90	2.87	1.587	2795.544	1.61	0.79	<i>0.29</i>	0.73	2.20	1.384	2802.702
24194	0.50	2.13	0.82	<i>0.31</i>	0.87	2.82	1.549	2795.652	1.63	0.79	<i>0.29</i>	0.74	2.21	1.377	2802.811
24249	0.66	2.15	0.80	<i>0.33</i>	1.01	2.64	1.763	2795.723	1.75	0.80	<i>0.29</i>	0.81	2.29	1.445	2802.813
24250	0.66	2.16	0.84	<i>0.33</i>	0.99	2.73	1.721	2795.749	1.84	0.81	<i>0.30</i>	0.85	2.39	1.481	2802.880
24290	0.82	2.43	0.81	<i>0.30</i>	0.80	3.30	1.437	2795.829	1.78	0.79	<i>0.29</i>	0.73	2.46	1.361	2802.983
24291	0.82	2.32	0.81	<i>0.30</i>	0.85	3.11	1.512	2795.877	1.80	0.79	<i>0.29</i>	0.78	2.40	1.415	2803.020

^a fluxes are in units of 10^{-11} erg s⁻¹ cm⁻²

^b *I*(p) (source intensity) is in units of 10^{-11} erg s⁻¹ cm⁻² Å⁻¹

with the gaussian broadening

$$f_2(s, \lambda) = \frac{1}{\sqrt{2\pi}s} \exp[-(\lambda - \lambda_0)^2/2s^2]. \quad (2)$$

Here, I_b is the background flux level, from which the profile is measured. I_0 is an assigned source flux level, subject to redistribution from the scattering atmosphere. In our integration of the profile we make use of integrals J_1 and J_2 to form the basic rotational ('dish-shaped') profile f_1 (cf. e.g. Budding and Zeilik, 1994, and for further background to the terms used cf. Oláh et al. (1992)). This description appears adequate for optically thin conditions.

When we take into account scattering, however, we replace f_2 with f_3 , which integrates emerging flux down to an optical depth ' τ ' at the line centre:

$$f_3(\tau, s, \lambda) = (1 - \exp[-\tau f_2])/\tau. \quad (3)$$

The form f_2 is now regarded as the limiting case of line-broadening by turbulently moving contributors in an optically thin regime. The form f_3 assumes a photon flux from such contributors to have undergone scattering by as much as a representative optical depth ' τ ' at the wavelength of the line centre. The ratio of the h to the k line flux indicated a non-optically thin medium transferring the Mg II lines to the features we observe (see Fig. 5).

We then proceeded to trial this 3-parameter fitting function. We found a strong correlation to exist, particularly affecting the values of ' r ' and ' τ '. This can be understood in terms of finite optical depth tending to flatten out the line centre, in a way comparable to the flattening of the dish-shaped effect, due to rotation. These effects will tend to counter each other. Such results demonstrate the rather limited extent of real, quantitative information often characterizing practical curve-fitting studies with independent parameters. Because of the strong correlation involving the ' r ', ' s ', and ' τ ' parameters we would keep one of them fixed in later trials. First, we set $\tau = 0.8$, as indicated

by the h to k line ratio results, and derived a mean $r=0.29\text{Å}$ from the fittings to all the Mg II lines. Since the rotation rate would not, in fact, change, we then adopted this value and used subsequent fittings to examine optimal values of ' s ' and ' τ '. We note here that the correlated error estimates of ' τ ' are large (0.3-0.4), though its value tends always to be around 0.8.

4. Results

The final results of modelling the 'clean' emission line data (wavelengths, peak intensities, ' τ ' and ' s ' parameter values and fluxes) are given in Table 1 along with the FWHM values resulted from the two-Gaussian fit. We give ' r ' parameter values in italics, since they result from the first round when the optical depth parameter was kept fixed. These values formed the mean ' r ' parameter value used in the final fit. The other fitted parameters (except FWHM) are from the final fitting.

The fit of the 'clean' lines are given in Fig. 2 for the same spectra as of Fig. 1. A slight difference is seen between the h&k lines in the red side of the original as well as in the clean spectra, i.e., the k line wing seems to be redshifted by about 10 km s^{-1} relative to the h line wing. Robinson and Carpenter (1995) have found this effect in a large number of giant stars.

The corresponding parameters' values are displayed in Fig. 3 (panels b, c, d), together with the V band light curve (panel a). Flux values from Dempsey et al. (1996a) (stars) are also plotted for comparison. This comparison shows a good agreement between two different processes used for flux determination. Dempsey et al. (1996a) combined two spectra at each phase before measuring while we processed pairs of spectra of the same phase separately.

We have calculated the artificial modulation of the flux originating from the interstellar absorption (see Houdebine et al., 1994). This artificial flux modulation is a double peaked curve resulting from the similarity between IM Peg's system velocity of -13 km s^{-1} , deduced from the present observations, and the

MgII h&k lines

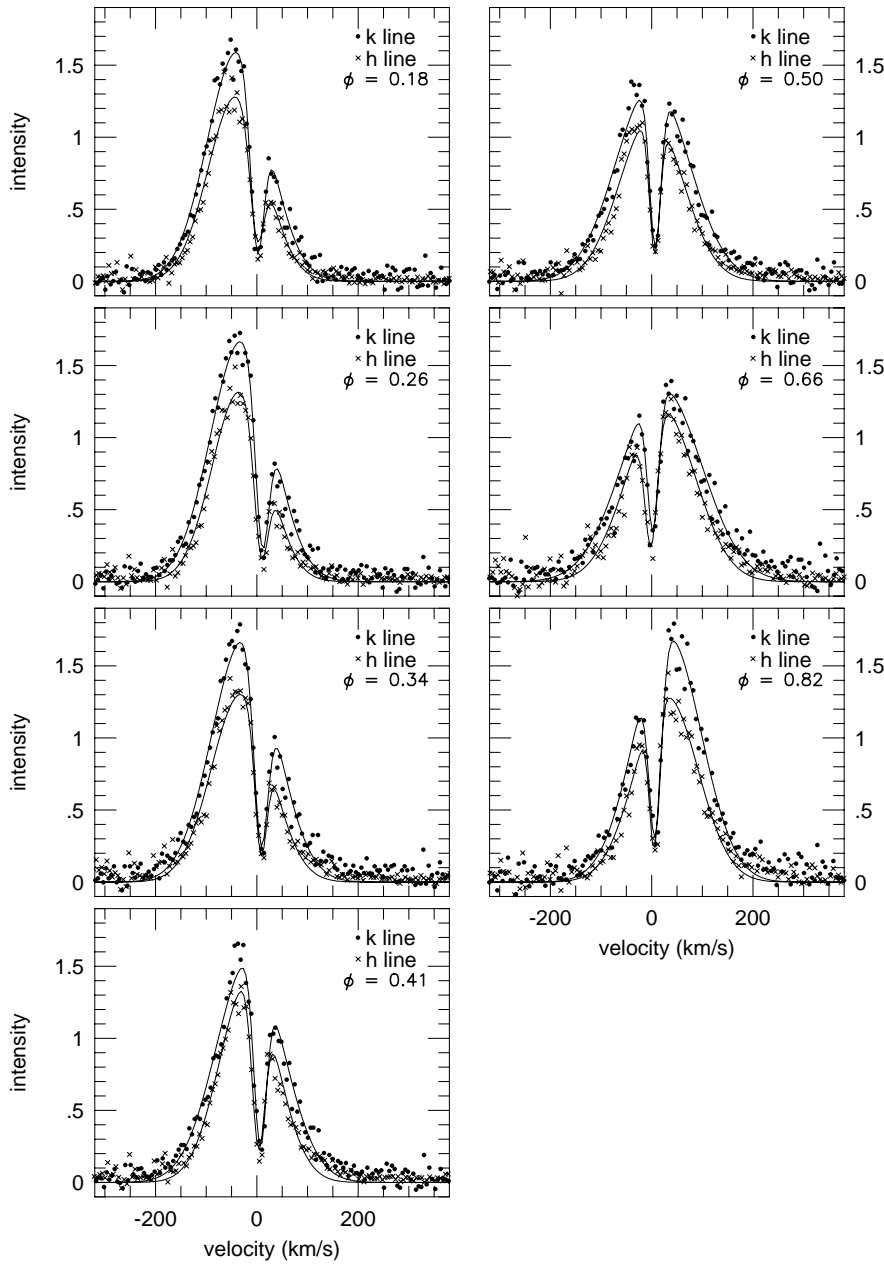


Fig. 1. IUE LWR observing data of IM Peg and the two component Gaussian fits for 7 spectra (uncleaned). These spectra cover almost one rotational cycle. Intensities are in units of $10^{-11} \text{ erg s}^{-1} \text{ cm}^{-2} \text{ \AA}^{-1}$

velocity of the interstellar medium in the direction of the star, which is $\approx -6 \text{ km s}^{-1}$ (Böhm-Vitense, 1981). Our measurements give $+7 \pm 6 \text{ km s}^{-1}$ from the average wavelengths of the Mg II h and k IS lines. According to our calculations, however, the artificial modulation makes up only about 1.4% of the flux variability.

For comparison, other activity indicators observed near the same time by IUE and $\text{H}\alpha$ are plotted in Fig. 3 from Dempsey et al. (1996a; note their Figs. 7 and 14 are swapped). The chromospheric and transition region line fluxes, strength of $\text{H}\alpha$ and the ‘s’ parameter of the Mg II lines run completely parallel.

We find mean Gaussian (turbulent+other: see the description of the ‘s’ parameter in Sect. 3) broadening widths of 75 and

85 km s^{-1} for the h and k lines, respectively, which may be compared with 2 km s^{-1} thermal velocities. These widths attain $85\text{--}110 \text{ km s}^{-1}$ when the maculation is close to the greatest and fall to close to $65\text{--}75 \text{ km s}^{-1}$ half a cycle later.

4.1. The rotational broadening

The rotational broadening ‘r’ parameters of the h and k lines are on average 0.28 \AA (30 km s^{-1}) and 0.30 \AA (32 km s^{-1}), respectively (Table 1.). The difference between the two values cannot be taken as real because of the typical error of their determination of 0.01 \AA .

MgII h&k lines

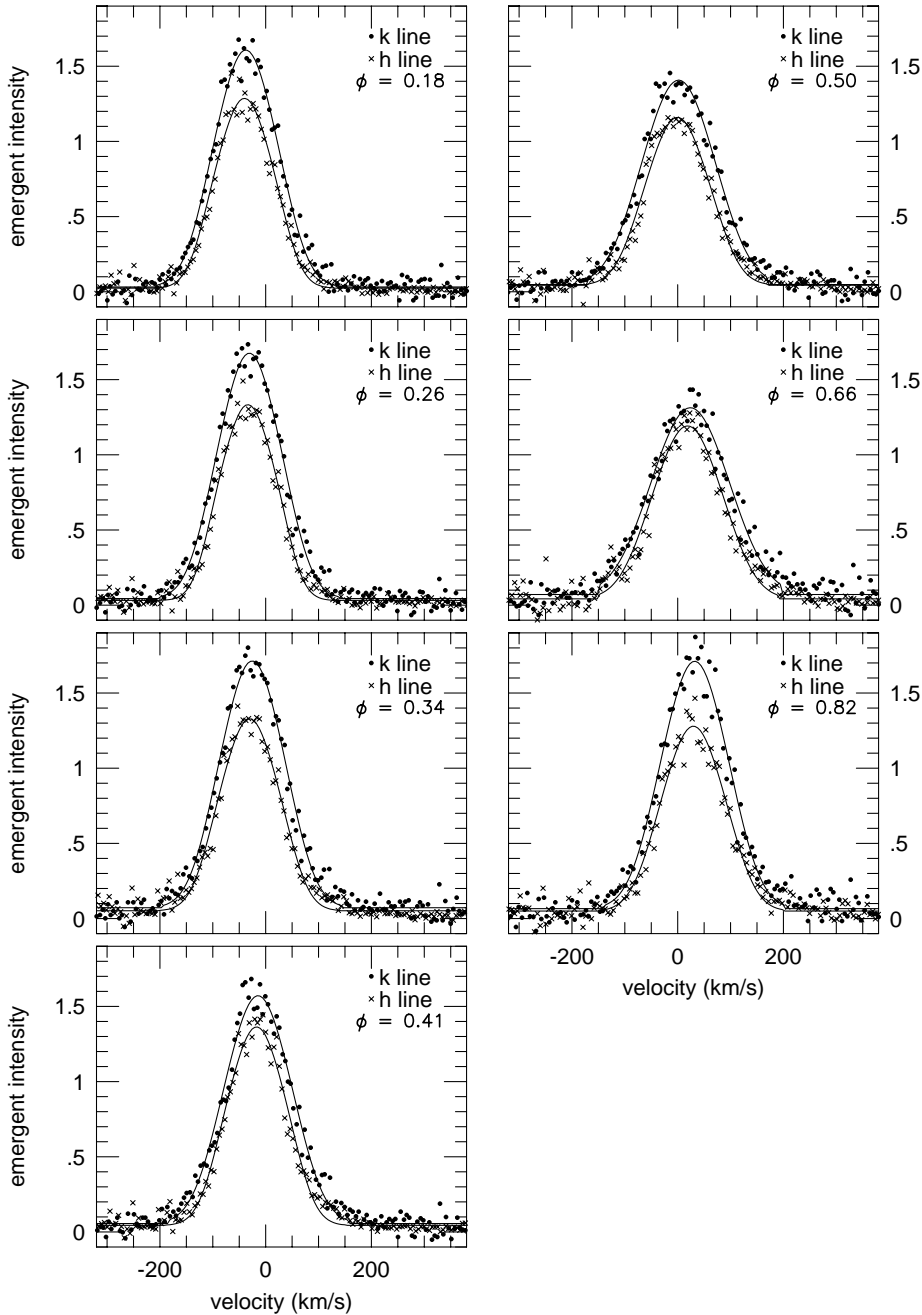


Fig. 2. The final fit of the clean lines (data and model). Intensities are in units of 10^{-11} $\text{erg s}^{-1} \text{cm}^{-2} \text{\AA}^{-1}$

The reliability of the rotational broadening parameter can be assessed knowing the star's rotational period and radius using $v_{rot} = 2\pi R/P_{rot}$. For IM Peg $P_{rot} = 24.649$ days, and its radius can be taken to be between $16\text{--}20R_{\odot}$ in accordance with its spectral type of K2II–III (Cowley and Bidelman, 1979), which yields $33\text{--}41 \text{ km s}^{-1}$ for v_{rot} . Taking $i = 56^{\circ}$ from Stawikowski and Glebocki (1994), and using $16\text{--}20R_{\odot}$ we get $27\text{--}34 \text{ km s}^{-1}$ for $v \sin i$. On the other hand, from an average ‘r’ parameter of the h&k lines of 0.29\AA we get $v \sin i \approx 31 \text{ km s}^{-1}$, in good agreement with the preceding values, taking into account the uncertainties in both the inclination and radius of the star. Fekel (1986)

gives $v \sin i = 28.2 \text{ km s}^{-1}$ measuring the FWHM of a few lines around the 6430\AA spectral region. With the same fitting function as ours for modelling rotational broadening, Huisong and Xuefu (1987) obtained $v \sin i = 36 \text{ km s}^{-1}$ for IM Peg from two iron and one calcium lines around 6700\AA .

5. Discussion

The magnesium resonance doublet is a powerful diagnostic of stellar outer atmospheres because it permits a differential optical depth analysis. In the optically thin case, the line shapes are almost identical and the h to k flux ratio throughout the profile

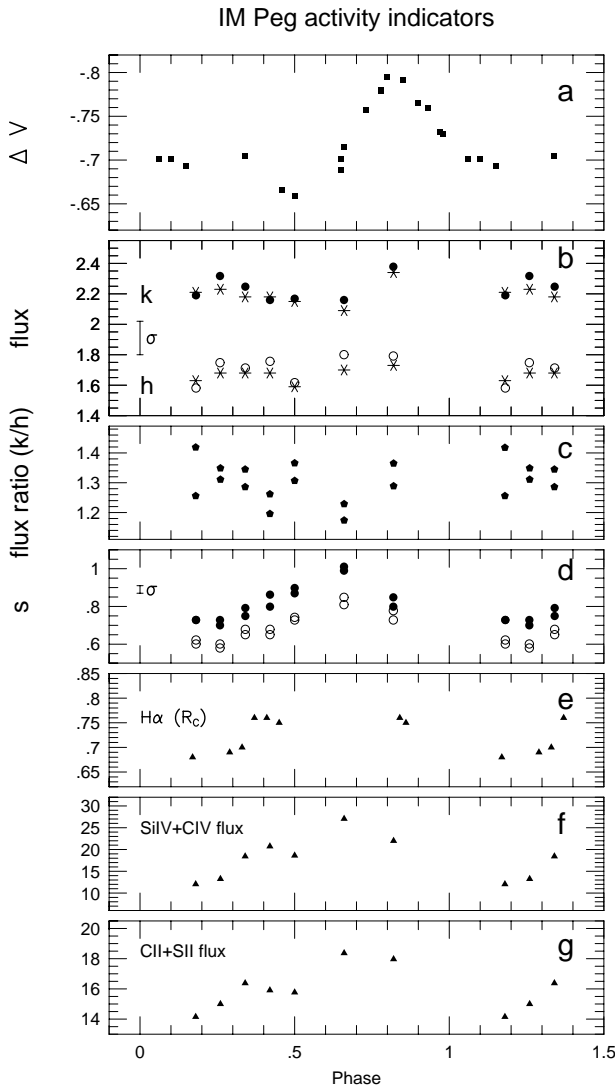


Fig. 3a–g. Resulting parameters of the ‘clean’ fits of the Mg II h&k line together with the V band light curve supplemented with other activity indicators observed near the same time in the short wavelength region and in H α . Symbols: filled squares: V observations, dots: k line parameters, circles: h line parameters, stars: fluxes from Dempsey et al. (1996a), filled stars: flux ratio, filled triangles: other activity indicators from Dempsey et al. (1996a). Units in the different panels are: **a** mag., **b** 10^{-11} erg s $^{-1}$ cm $^{-2}$, **c** dimensionless, **d** Å, **e** residual line core intensity, see Dempsey et al. (1996a), **f** and **g** 10^{-13} erg s $^{-1}$ cm $^{-2}$. On the left side of panels **b** and **d** the average standard deviations of the resulting parameters are shown

equals the ratio of the oscillator strengths (0.5). For the optically thick case the ratio tends towards unity. In real cases, however, the optical depth varies along the line profiles, being commonly larger at line center and smaller in the wings. Directly comparing the line profiles is therefore a potential diagnostic of the optical depth.

First, let us investigate the main spectral characteristics of the Mg II doublet of IM Peg. The h&k line fluxes and widths display significant variations throughout the orbital phase; the k

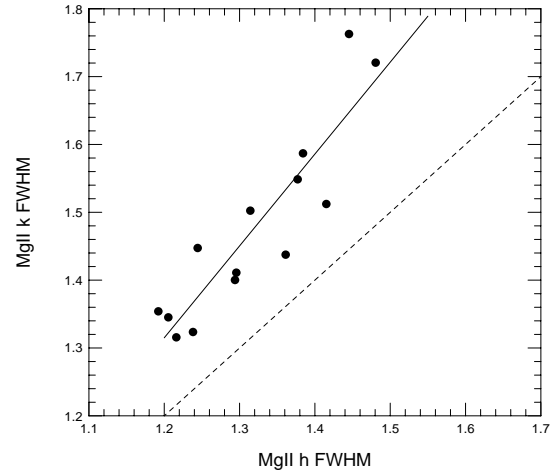


Fig. 4. The k line width as a function of h line width, in angströms

flux reaches a maximum when the star is brightest around phase 0.8, but previous to this, it shows a progressive fall (phase 0.2 to 0.65). During the decrease of the k line flux, both the h and k line widths increase, while the h line flux remains more constant (Fig. 3, panels b and d). These changes are unambiguous signatures of the varying properties of the emitting medium.

In Fig. 4 we show the k width as a function of the h width. Both widths should correlate because broadening mechanisms (turbulence, rotation, radiation transfer) affect both lines simultaneously. We do observe some correlation (Fig. 4) but with a scatter consistent with measurement uncertainties. The slope of the correlation remains greater than unity, which is evidence for radiation transfer effects (i.e. radiation damping that occurs when a line is not optically thin) and a non-optically thin medium at all phases. The correlation can be given by the following linear relation:

$$\text{FWHM}(k) = 1.351(\pm 0.186)\text{FWHM}(h) - 0.307(\pm 0.246) \quad (4)$$

That the slope is typically larger than 1 by 10% is another indication for larger radiation transfer effects in the k line, where the optical depth is twice as large as in the h line. However, if this rise in broadening was due to radiation transfer alone, it should be correlated to changes in the k to h line flux ratio, but this is not convincingly observed. Only at the k flux minimum does the line width increase and the flux ratio decrease significantly; see Fig. 3 (panels b,c,d). The possible reason for this result, beside measurement uncertainties, is that the difference in line widths is partly due to radiation transfer, but the increase in the widths is due to turbulence and/or rotation (extended structures). It seems that the magnesium line optical depths in their region of formation is on average larger at the k line minimum.

The ‘ τ ’ parameter perhaps shows a slight wave as the star rotates (see Table 1.), parallel with the other activity indicators, which may signify variable optical depth, but because of the large error of the determination we cannot take these changes as evidence.

The real situation is probably more complex than we describe. However, we believe that in the simplest understanding

MgII h/k

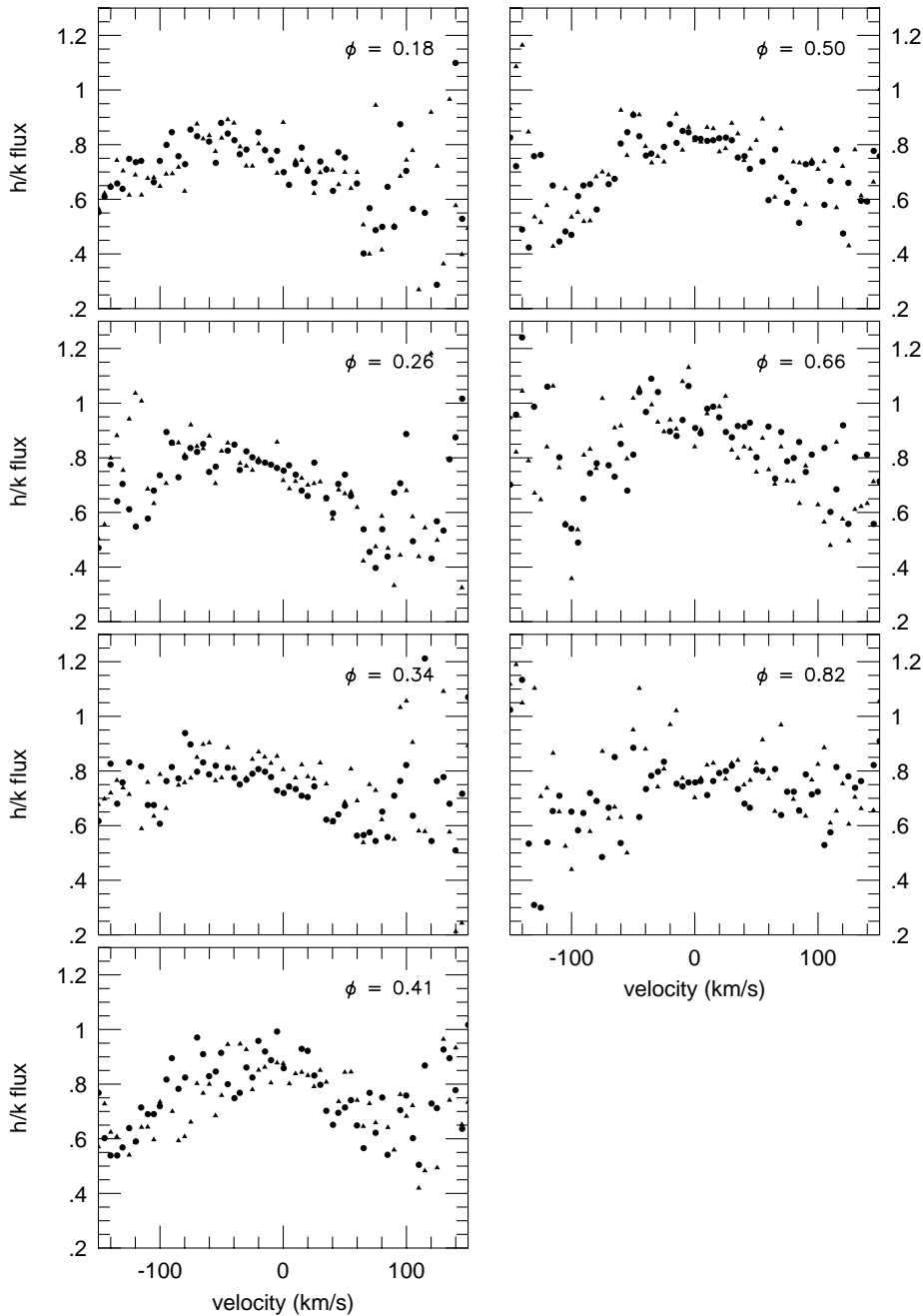


Fig. 5. The ratio of the h line to the k line flux for different phases. Dots and triangles represent the longer and shorter exposure spectra, respectively. A ratio of 1 and 0.5 correspond respectively to the optically thick and optically thin cases

of the situation one would expect the line centre to provide the most sensitive measure of the optical depth and test of our understanding of possible broadening effects.

The ratio of the h to k line fluxes is displayed in Fig. 5. This ratio should lie between 1 (optically thick) and 0.5 (optically thin), and should diminish from the line core to the wings. This is verified up to about 100 km s^{-1} into the wings, but then the ratio starts increasing up to a value of 1 where the line contribution becomes zero. This later increase is an artifact due to the incorrect fit into the wings where the flux is very small. We shall therefore consider only the profiles between -100

to 100 km s^{-1} : there we observe a systematic asymmetry that never reverses. This asymmetry could be due to a larger optical depth on the red wing from active regions disappearing on the receding limb, although this scenario is rather improbable.

There are significant changes occurring in the h to k line ratios (Fig. 5); for instance, the flux ratio at line center is substantially larger at phases 0.41 and 0.66 when it reaches almost 1, which corresponds to low k fluxes and generally larger line widths. This is consistent with higher density plasmas and optical depths. The profile at phase 0.82 is much flatter, also indicating larger optical depths, but at this time in the wings rather

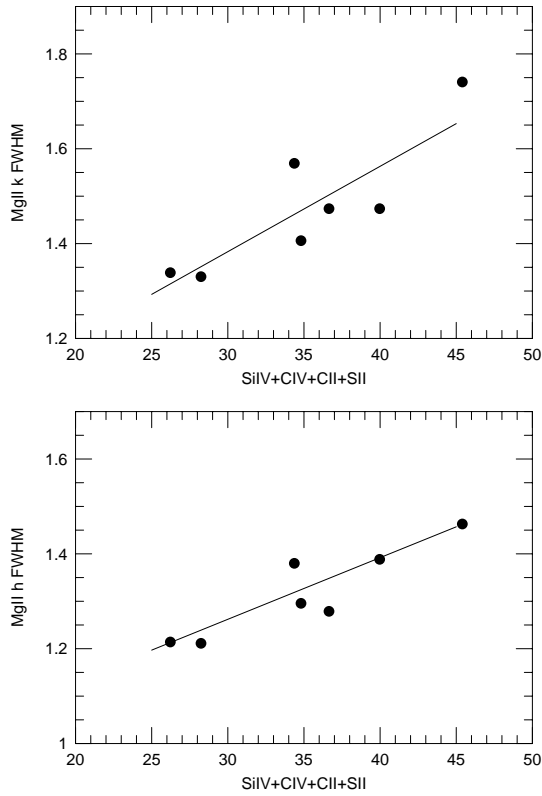


Fig. 6. Average of the h&k line widths as a function of the sum of the Si IV, C IV, C II, and S II line fluxes

than at the line center. The lack of phase coverage does not allow us to understand fully the origin of the large changes that occur on the surface and/or in the chromospheric structures, but the Mg II line characteristics emphasize that the outer atmosphere is quite inhomogeneous.

We also found that the Mg II line widths ($W(\text{Mg II})$) increase with higher temperature line fluxes ($F(\text{SWP})$, the sum of Si IV + C IV + C II + S II lines), as shown in Fig. 6, and follow the relations:

$$W(\text{MgII})(h) = 0.013(\pm 0.003)F(\text{SWP}) + 0.872(\pm 0.109) \quad (5)$$

$$W(\text{MgII})(k) = 0.018(\pm 0.006)F(\text{SWP}) + 0.843(\pm 0.197) \quad (6)$$

Wood, Linsky & Ayres (1997) have found a related correlation between the width of their ‘broad’ Gaussian component of the C IV lines of several stars and their X-ray surface flux. Unfortunately, X-ray observations obtained simultaneously with those reported here were not obtained.

The maximum flux in the higher temperature lines is attained when the k line flux is at minimum (Fig. 3, panels b, f, g) and the visual brightness is at maximum. Because these lines are probably optically thin and their formation is collisionally controlled, their fluxes are expected to increase with electron density. It is also important to note the correspondence between the chromospheric and photospheric diagnostics; maximum widths in the Mg II profiles are reached at about the assumed maximum spottedness (light minimum), while the maximum flux occurs at minimum spottedness.

Table 2. Results of the radial velocity measurements

HJD	phase	RV km s ⁻¹	O–C km s ⁻¹	Obs./Templ.
2448536.7863	0.9062	22.27	0.83	NSO α Ari
2448537.8484	0.9493	21.38	-0.58	NSO α Ari
2448558.8707	0.8022	10.84	1.05	NSO α Ari
2448560.8660	0.8831	20.25	0.22	NSO α Ari
2448571.7414	0.3243	-41.31	-1.54	NSO α Ari
2448572.6619	0.3617	-41.09	2.28	NSO α Ari
2448573.7117	0.4043	-45.39	0.12	NSO α Ari
2448582.8332	0.7743	2.88	-1.95	NSO α Ari
2448583.6330	0.8068	12.06	1.51	NSO α Ari
2448584.6584	0.8484	16.89	0.34	NSO α Ari
2448594.6694	0.2545	-29.93	-0.72	NSO α Ari
2448598.6300	0.4152	-46.84	-1.12	NSO α Ari
2448644.6405	0.2818	-33.44	0.44	NSO α Ari
2448647.6218	0.4028	-46.04	-0.57	NSO α Ari
2448657.6336	0.8090	12.22	1.31	NSO α Ari
2448631.6420	0.7545	-1.94	-2.95	NSO α Ari
2448026.9380	0.2217	-22.66	0.19	KPNO α Boo
2448026.9644	0.2227	-22.68	0.39	KPNO α Boo
2448029.9506	0.3439	-44.19	-2.34	KPNO μ Her

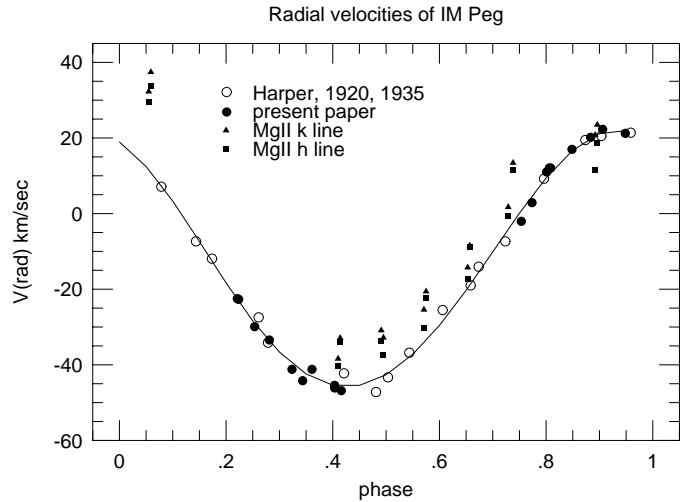


Fig. 7. Radial velocity curve of IM Peg from Harper (1920), and using the velocities of Table 2. Mg II h&k velocities are also displayed. See the text for explanation

Hence, all spectral diagnostics, apart from the k to h flux ratio which is inconclusive, suggest the progressive appearance on the stellar disc of a higher pressure formation. Higher pressure possibly means a higher magnetic field strength produced by active regions (see Golub et al. 1980) indicating the presence of at least one major plage area.

6. New orbit of IM Peg

Fig. 7 gives the radial velocity curve of IM Peg observed by Harper (1920, 1935). Our measurements of radial velocities have also been plotted on this diagram.

Table 3. New orbital elements of IM Peg

element	$\gamma(\text{km s}^{-1})$	$K(\text{km s}^{-1})$	e	ω	$T_0(\text{HJD})$	P(days)
Harper	-12.84	33.20	0	-	2422240.992	24.65
1920	± 0.34	± 0.49	-	-	± 0.054	-
present	-12.985	33.944	0.0372	24.9001	2422238.8693	24.6487620
paper	± 0.356	± 0.488	± 0.0127	± 22.6689	± 1.5599	± 0.0001064

To calculate an improved orbit we measured 19 new radial velocities using the cross-correlation method described in Bopp & Dempsey (1989). Sixteen spectra covering the 6380-6440Å region were obtained with the National Solar Observatory (NSO) McMath telescope utilizing a Milton-Roy grating (1200 lines/mm) in second order with an 800×800 TI CCD (15 μm pixels). All spectra were obtained in the fall of 1992. The spectra have a 2 pixel resolution of 0.19Å and S/N of greater than 200:1. Three additional spectra of the same region but with a 2 pixel resolution of 0.22Å were obtained with the Kitt Peak National Observatory (KPNO) coude feed telescope utilizing the 1024×1024 TIKKA CCD (27 μm pixels), grating A and camera 5. The S/N was 100-200:1. For the NSO data the template star was α Ari (K2 III, $V = -14.3 \text{ km s}^{-1}$). For the KPNO data the templates were α Boo (K2 III, $V = -0.04 \text{ km s}^{-1}$) and μ Her (G5 IV, $V = -15.6 \text{ km s}^{-1}$). Errors in the resulting radial velocities result primarily from the accuracy of the wavelength comparison spectrum usually obtained before and after the stellar spectra. Based on previous results (Bopp & Dempsey 1989) we estimate the errors to be less than 1 km s^{-1} . Measurements obtained with different standard stars available and between template stars show agreement to within 0.3 km s^{-1} . Results are listed in Table 2.

A new orbit was derived by use of standard least-squares fitting programs (Bopp, Evans & Laing 1970). Our values were combined with those of Harper (1920) to obtain the final orbit. According to Harper (1920), errors for the older data were 20% larger than ours and were therefore given a weight of 0.8 while the modern values were equally weighted at 1.0. The final elements are listed in Table 3. Our orbit agrees very well with that of Harper (1920) although we derive a small, but non-zero eccentricity.

The velocities of the Mg II h&k lines have a systematic offset of about $+15 \text{ km s}^{-1}$ with respect to the radial velocity curve, and the error of these velocities are quite high, about 5–8 km s^{-1} . This offset is very probably of instrumental origin, if not, than perhaps this reflects global flows on the star. The same effect was found on EI Eri by Neff (1991), who gave these possible explanations of the observed offset of the star's Mg II h&k line velocities.

7. Conclusions

We have determined an optimal line of sight rotation velocity of 31 km s^{-1} , which is in keeping with other published values to within published or expected errors. We find also representative mean Gaussian (turbulent+other) broadening widths of

80 km s^{-1} for both the Mg II h&k lines. These widths vary by about 25% as the star rotates, following closely (but not matching) the maculation wave. We find a net redward shift of the Mg II emission lines with respect to the underlying star of about 15 km s^{-1} . There is also a redward shift of the k line wing by about 10 km s^{-1} relative to the h line.

From the line profile modelling we can draw further conclusions:

- The width of the Mg II k-line is 10% larger, but well correlated with, that of the h-line width.
- The asymmetry in the ratio of the Mg II line flux suggest a difference in the optical depth in the redward line forming region.
- The values of ‘ τ ’ resulted from the h to k line ratios and determined in the fittings support each other.
- The width of the Mg II h&k resonance lines increases as the flux of higher temperature emission lines also increases, both of which vary significantly during the rotational period.
- The flux of the transition region lines as well as the C II and S II emission appear to peak around light minimum, i.e., spot maximum.
- Variations of the line profile parameters seen as a function of phase, suggest the preese of a discrete, high pressure region moving across the stellar disk as the star rotates.

Although not conclusive, the above points suggest that a plage was detected on the primary of IM Peg. Since the flux of the transition region lines as well as the C II and S II emission appear to peak around light minimum, i.e., spot maximum, the plage may well be associated with cooler spots as observed in the solar paradigm.

Finally, a revised orbit has been calculated showing good agreement with Harper’s 1920 result, although we do find evidence for a small, but real, eccentricity.

Acknowledgements. The authors wish to thank P. Avellar and M. Giampapa for the NSO Synoptic Program data used in this paper. Thanks are due to our late referee, P.B. Byrne, whose remarks helped to improve this paper considerably. We are grateful to Zs. Kóvári, B. Szeidl and I. Vincze for helpful discussions. This research was partly supported by the Hungarian Research Grant OTKA T-015759 and T-019640. Research at CSC has been supported by NASA grant NAS5-32616.

References

- Bopp, B. W. and Dempsey, R. C. 1989, *PASP*, 101, 516
 Bopp, B. W., Evans, D. S., Laing, J. D. 1970, *MNRAS*, 147, 355
 Böhm-Vitense, E. 1981, *ApJ* 244, 504

- Budding, E. and Zeilik, M. 1994, Ap&SS 222, 181
Cowley, A.P. and Bidelman, W.P. 1979, PASP 91, 83
Dempsey, R.C., Neff, J.E., O'Neal, D., Oláh, K. 1996, AJ 111, 1356
Dempsey, R.C. et al. 1996, ApJ 470, 1172
Dempsey, R. C. et al. 1997, in: Cool Stars, Stellar Systems, and the Sun 10, ASP Conference Series, eds B. Donahue & J. Bookbinder, in press
Eaton J. et al. 1983, A&SS 89, 53
Fekel, F. C. 1997, PASP 108, 514
Golub, L. et al. 1980, ApJ 238, 343
Harper, W.E. 1920, Publ. DAO 1. 203
Harper, W.E. 1935, Publ. DAO 6. 251
Houdebine, E.R., Doyle, J.G., Butler, C.J. 1993, Irish Astr. J. 21, 102
Huisong, T. and Xuefu, L. 1987, A&A 172, 74
Neff, J.E. 1991, in: Surface Inhomogeneities on Late-Type Stars, ed. Byrne and Mullan, Lecture Notes in Physics No. 397, p. 54
Neff, J.E., Walter, F.M., Rodono, M., Linsky, J.L. 1989, A&A 215, 79
Oláh, K., Budding, E., Butler, C.J., Houdebine, E., Gimenez, A., Zeilik, M. 1992, MNRAS 259, 302
Robinson, R.D. and Carpenter, K.G. 1995, ApJ 442, 328
Stawikowski A., Glebocki R. 1994, Acta Astr. 44, 393
Wood, B.E., Harper, G.M., Linsky, J.L. & Dempsey, R.C. 1995, ApJ 458, 761
Wood, B.E., Linsky, J.L. & Ayres, T.R. 1997, ApJ, submitted
- This article was processed by the author using Springer-Verlag L^AT_EX A&A style file L-AA version 3.